Mapping wetland areas on forested landscapes using Radarsat-2 and Landsat-5 TM data

Jennifer Martin

Arbetsrapport 382 2012
Masters thesis

Handledare:
Heather Reese

Sveriges lantbruksuniversitet
Institutionen för skoglig resurshushållning
Utgivningsår: 2012

ISSN 1401–1204
ISRN SLU–SRG–AR–382

Mapping wetland areas on forested landscapes using Radarsat-2 and Landsat-5 TM data

Jennifer Martin

Master's Thesis completed through the TRANSFOR-M program with University of New Brunswick, UNB and Swedish University of Agricultural Sciences, SLU.

EX0627
Supervisor: Heather Reese, SLU, Department of Forest Resource Management, Remote Sensing
Examiner: Johan Fransson, SLU, Department of Forest Resource Management, Remote Sensing
External supervisor: Professor Brigitte Leblon, University of New Brunswick and Dr. Kara Webster, Natural Resource Canada

Sveriges lantbruksuniversitet
Institutionen för skoglig resurshushållning
S-901 83 UMEÅ
www.srh.slu.se
Tfn: 018-671000

ISSN 1401–1204
ISRN SLU–SRG–AR–382–SE

Abstract

Wetlands are an important ecosystem for many vital functions such as groundwater recharge, flood control, water quality improvement, and to mitigate erosion. Monitoring and mapping wetlands on a large scale is becoming increasingly more important, and satellite remote sensing provides a practical approach. This study examines the potential for using multi-beam Radarsat-2 C-band polarimetric SAR, Landsat-5 TM, and DEM data for classifying wetland and non-wetland classes in a forested watershed in Ontario, Canada. It investigates the influence of incidence angle, leaf presence and moisture conditions in the classification of SAR images. The images were classified using two classification methods: the Maximum Likelihood Classifier and Random Forests classifier. Lastly, SAR polarimetric variables and decompositions were investigated for their usefulness in classification.

Fourteen Radarsat-2 Fine Quad (FQ) SAR images were acquired from October 2010 to November 2011 at different incidence angles but with the same orbit-descending pass (west-looking direction). The images were paired according to the beam mode (FQ4 and FQ22/27), leaf presence (off and on) and moisture (wet/dry) conditions. The FQ image pair which gave the best classification overall accuracy (76.3%) using the Maximum Likelihood classification was those from the two FQ22/27 images acquired under leaf-off and dry conditions. When the FQ images were classified together with five optical bands of a Landsat image, the classification accuracy was higher for all classes as well as for the overall accuracy (94.4%). When the FQ images were combined with the Landsat image and slope, overall accuracy improved only slightly from the FQ and Landsat combination (95.4%).

With the Random Forests classification, the best overall accuracy was obtained with the combination of the FQ 22/27 image pair acquired under leaf-off and dry image conditions, Landsat and slope (98.7%), followed closely by the FQ pair and Landsat combination (98.6%). When all FQ images were used as input to the Random Forests classification, this also produced high cross-validation overall accuracies (98.3%), indicating that while Landsat does add accuracy FQ images can give comparable accuracies if the right dates and conditions are chosen. A benefit of using Random Forests is the ability to rank band importance in image classification. From this it was determined that using multiple FQ images with leaf-off conditions were preferred. As for the other conditions, a mix of incidence angles, moisture conditions, and polarizations were important for classification. The incoherent target decompositions were the most important polarimetric variable in the classification, while the only other parameter indicated as important from both classifications was the orientation angle for the maximum of the completely polarized component.

In future studies, it may be of interest to test the combination of multi-date polarimetric variables and decompositions parameters together with all polarizations (HH, HV, VH, and VV). So far, we classified only two types of wetlands (closed and open). Further studies are needed to test the Random Forests classifier for classifying the wetlands into more detailed classes (bog, fen, marsh, swamp, etc.). Lastly, future studies should test the results found here using independent evaluation data to assess the accuracy.

Keywords: Radarsat, Landsat, wetlands, classification, land cover, multi-source data, remote sensing, Random Forests, Maximum Likelihood Classifier

1. Introduction

1.1 Importance of the study

Wetlands are an important ecosystem as they perform a variety of functions that are beneficial to society and the environment. They are crucial for groundwater recharge, flood control, water quality improvement, and mitigate erosion (Li & Chen, 2005). Understanding the distribution and dynamics of wetlands are essential for understanding ecosystem diversity and function and how it is impacted by human practices and global changes. Monitoring and mapping wetlands in Canada is significant as wetlands cover 14% of Canada's land area (over 127 million ha; Cox, 1993) and make up 24% of the world's wetlands (Baghdadi et al., 2001). There is even increasing importance globally, as there has been extensive wetland loss in the last half century due to constant pressures for land use changes and development (Henderson & Lewis, 2008). Developing a mapping tool to extract information about wetland areas from satellite imagery is essential for mapping large scale regions. Satellite remote sensing has several advantages over other methods such as aerial photograph interpretation and ground surveys as they provide multi-temporal data over large area. The images are also relatively easy to acquire, and this is more cost-effective (Li & Chen, 2005). The use of satellite remote sensing technologies provide a practical approach to mapping wetlands in Canada, due to the vast areas that need to be mapped, most of which are in remote areas.

Optical images like those provided by Landsat and SPOT (Système Probatoire d'Observation de la Terre) satellites can be used, but image availability is limited to clear sky conditions. By contrast, synthetic aperture radar (SAR) images can be acquired whatever the cloud conditions. They should be suitable for wetland mapping as radar backscatter is sensitive to moisture conditions, because both depend on the dielectric properties of vegetation and soil (Henderson & Lewis, 2008). RADARSAT-2 is a C band SAR system that can acquire dual polarized (HH and HV, or VV and VH), multi-polarized images (HH, HV, VH, VV) as well as polarimetric images (multi-polarized images that have the phase information).

C-band has been shown to be useful in discriminating between forests and forested wetlands in leaf-off conditions (Henderson & Lewis, 2008) and can detect standing water under low vegetation (Henderson & Lewis, 2008; Li & Chen, 2005), such as marshes. Our study will test the use of multi-beam RADARSAT-2 multi-polarized images (HH, HV, VH, and VV) and polarimetric images (that include the phase information) for mapping wetland areas in forested regions in Ontario. The study also uses Landsat-5 TM and DEM data.

1.2 Wetlands

Wetlands are defined as "*land that is saturated with water long enough to promote wetland or aquatic processes as indicated by poorly drained soils, hydrophytic vegetation and various kinds of biological activity which are adapted to a wet environment* (National Wetlands Working Group, 1988). They are generally discrete entities between unsaturated upland and aquatic deep water, with the water table at or near the surface, or shallow water for most of the growing season (National Wetlands Working Group, 1997). Three basic elements in identifying wetlands include hydrophytic vegetation, hydric soils, and wetland hydrology. Hydrophytic vegetation consists of macrophytic plants that grow in water, soil,

or substrate that is at least periodically deficient in oxygen due to the presence of excess water. Hydric soils are soils that are saturated, or flooded long enough during the growing season to develop anaerobic conditions. Wetland hydrology exists in conditions of permanent or periodic inundation or saturated soils at the surface for at least part of the year (National Wetlands Working Group, 1997). Wetness for an area is influenced by precipitation, topography, soil permeability, and plant cover. Wetlands are saturated long enough to promote soil development and vegetation conditions that are adapted to saturated conditions.

The Canadian Wetland Classification System divides wetlands into five main classes based on genetic and environmental factors. The five classes are bog, swamp, fen, marsh, and shallow waters. Bogs are peat lands with generally raised or level surfaces. The water table is usually at, or slightly below the bog's edges. Bogs are typically acidic, and may have tree cover or not, and covered with Sphagnum moss and ericaceous shrubs. Swamps are forested wetlands with tall woody vegetation covering over 30% of the area. Generally the water table is below surface. They are not as wet as open wetlands (i.e. without trees, such as fen and marsh) and are comparable to bogs with tree cover. Fens are peatland forms with a fluctuating water table, where surface water may be present through channels or pools. The vegetation consists of predominantly sedge and brown moss, however it varies depending on water table level. When the water table is above surface, the vegetation consists generally of graminoids and some bryophytes. With a lower water table, shrubs are generally present, and trees can be present on drier fens. Marshes are distinguished by shallow waters that fluctuate. The water table may be at, or below soil surface, however, water usually remains within the rooting zone for most of the growing season. Vegetation mostly consists of rushes, reed grasses, and sedge and there is very little organic material or peat. Shallow waters are usually less than 2 meters at mid-summer. They are the transitional stage between lakes and other wetland types, and are free of vegetation (National Wetlands Working Group, 1997). Within the study area used in this thesis, the wetland classes found were mainly swamp (called "closed wetland" in this study) and fen and marsh (together called "open wetland" in this study).

1.3 Radar remote sensing of wetlands

Radar sensors are active sensors that operate in the microwave portion of the electromagnetic spectrum. Active sensors emit waves from their antenna, and record the "backscatter" of the imaged surface. Radar backscatter from a target is influenced by imaging geometry, topography, surface roughness, and dielectric constant (Lillesand et al., 2008). Unlike optical waves, microwaves are unaffected by clouds, can penetrate vegetation canopies to some degree. They are also sensitive to moisture and rainfall. Indeed, they are affected by the dielectric properties of the surface (soil and vegetation) that change with the moisture conditions (Henderson & Lewis, 2008). For example tonal differences between forests and clear cut are more prominent under wet conditions, as forested areas present rougher surfaces (Lillesand et al., 2008).

Radar signals can be transmitted and received in different polarization modes. Polarization refers to the orientation and shape of the pattern traced by the tip of the rotating electrical vector (E) of the electromagnetic wave. All the existing SAR sensors transmit and receive linear polarized waves, i.e., when the tip of E traces out a single line in the (X,Y) or (H,V) plane (H for horizontal and V for vertical). If E is parallel to the Earth's surface, then the

linear polarization is horizontal (H) (Figure 1a) and if it is perpendicular to the Earth's surface, then the linear polarization is vertical (V) (Figure 1).

The current SAR sensors can send and receive the H or V polarization, thereby there are four polarization combinations (HH, HV, VH, and VV) where the first letter represents the transmitted polarization and the second is for the received polarization. HH and VV are called co-polarizations, whereas HV and VH are cross-polarizations.

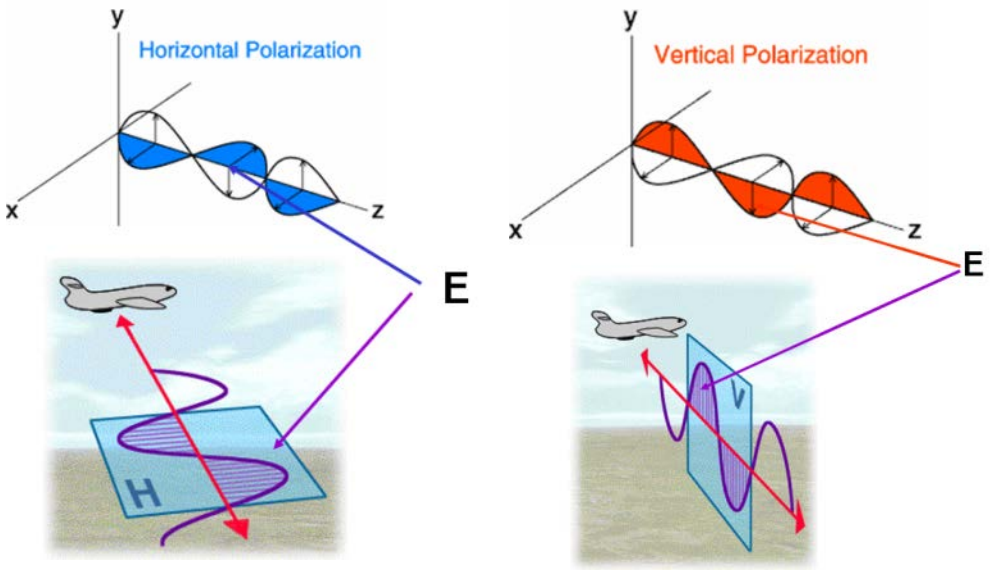

Figure 1. Radar horizontal (H) and vertical (V) wave polarizations. (CCRS, 2008).

Radar systems operate at different wavelengths, initially given an arbitrary letter code by the military for security reasons. Today they are still referred to by the same letter codes (Table 1).

Table 1. Radar band code and wavelength ranges

Band	**Wavelength (λ) range (cm)**
K_a	0.75 -1.1
K	1.1-1.67
K_u	1.67-2.4
X	2.4-3.75
C	3.75-7.5
S	7.5-15
L	15-30
P	30-100

Table 2 lists some of the existing SAR systems. The only systems which have a polarimetric mode are Radarsat-2, ALOS-PALSAR and Terra-SAR-X. This thesis uses Radarsat-2, which was launched in December 2007. It is a quad-polarization SAR system that has multiple beam modes, with a spatial resolution that can range from 3 m to 100 m, and the ability to be left – and right looking (CSA, 2007).

Table 2. Characteristics of the previous and existing spaceborne SAR sensors

Sensor(*)	**Band**	**Polarization**	**Incidence angle**	**Resolution (m)**	**Swath Width (km)**
ERS-1&2	C	VV	23 ^{o}	26	100
Radarsat-1	C	HH	10-59 ^{o}	10-100	50-500
JERS-1(*)	L	HH	38 ^{o}	18	75
Almaz(*)	S	HH	30-60 ^{o}	15-30	20-45
SEASAT	L	HH	20-26 ^{o}	25	100
ENVISAT	C	HH	15-45 ^{o}	30-1000	50-500
ASAR		VV			
		HH+HV			
		VV+VH			
		HH+VV			
SIR-C/X (*)	X	VV	15-50 ^{o}	30	15-60
SIR-C/L (*)	C, L	HH+VV+HV+VH	15-50 ^{o}	30	15-60
ALOS	L	HH	8-60 ^{o}	10-100	20-350
PALSAR(*)		VV			
		HH+HV			
		VV+VH			
		HH+VV+HV+VH			
Radarsat-2	C	HH	10-60 ^{o}	3-100	10-500
		VV			
		HH+HV			
		VV+VH			
		HH+VV+HV+VH			
TerraSAR-X	X	HH	20-55 ^{o}	1	5-100
		VV			
		HV			
		VH			
		HH+HV			
		VV+VH			
		HH+VV+HV+VH			

(*) does not exist anymore; the SIR-C systems were temporary missions on board of the Space Shuttle

Radar also has the ability to penetrate vegetation canopies to some degree, which varies with the wavelength band. Longer wavelength (10-30 cm) bands such as L and P- bands have the ability to penetrate through the canopy to tree trunks, while shorter wavelengths may not be able to fully penetrate the canopy, and can vary with canopy density, canopy volume, structure of canopy and species composition (Townsend, 2002). Radar backscatter is a function of geometrical factors relative to sensor and terrain, such as surface roughness, incidence angle, wavelength, and dielectric factors, such as the nature and moisture content of terrain. Surface roughness is expressed by the root mean square height of surface variation that depends on the wavelength and the incidence angle (Lillesand et al., 2008). For smooth surfaces, the radar beam is specularly scattered in one single direction, so the imaged surface appears dark on the SAR image.

Water is an example of a surface that can be smooth and thus often appears dark on the image. For rough surfaces, the radar beam diffuses in all directions and the imaged surface appears brighter on the SAR image. Double-bounce scattering can occur when a beam is spectrally reflected off a smooth horizontal surface to a vertical surface, resulting in a strong return. This is the case of flooded forests, where the radar beam is reflected from the water to tree trunks (Henderson & Lewis, 2008). Volume scattering occurs when the radar beam penetrates more than just the surface of the target, for example when it penetrates the vegetation canopy. The penetration is higher in the absence of leaves, which result in high backscatter of leaf-off deciduous trees (Baghdadi et al., 2001).

Table 3 summarizes some early literature results on the suitable frequencies and polarizations for wetland mapping with SAR imagery as a function of wetland types. Wetland classification can be improved through the use of multiple polarizations as opposed to single polarized imagery (Ozesmi & Bauer, 2002; Wang et al., 1998). Changes in polarizations result in changes in backscatter, and multiple polarizations can provide more information than a single polarization alone, especially when there is a specific orientation to an object or objects being detected. In the case of wetlands, when there is emergent vegetation within wetlands, L-VV return decreases while HH and VH returns rise (Ramsey et al., 1999). C-HH data was found to be superior to HV or VV data in delimiting flood extent, although HV data provides some information in regard to flood detection (Henry et al., 2006). According to Pope et al. (1997), C-HH data provided the highest accuracies for delimiting sawgrass and cattails, but C-VV data are useful to separate cattails and low-density marshes. Co-polarizations (HH and VV) give a higher contrast backscatter between swamps and dry forest than cross-polarization for X- and L-bands, which gives the ability to separate between flooded and non-flooded forests (Henderson & Lewis, 2008).

However, some studies have noted that cross-polarization is better at separating between marsh and swamp classes for L-band (e.g., Henderson & Lewis, 2008). The P- and L-bands have been useful in detecting standing water under forest canopies, as the surface water under forest canopies results in a double bounce and enhances the signal response. C-band data have been useful in detecting standing water under short vegetation (Henderson & Lewis, 2008: Li & Chen, 2005). C-band and X-band data have also been shown to be favorable in some wooded wetlands with low density canopies, or leaf off conditions (Henderson & Lewis, 2008; Townsend, 2002).

Table 3. Suitable frequencies and polarizations for wetland mapping with SAR imagery as a function of wetland types

Wetland type	**Band**	**Polarization**	**Authors**
Forests, dense vegetation	P, L		Kasischke & Bourgeau-Chavez,1997
Bog and inundated vegetation	L	HH	Yamagata & Yasuoka, 1993
Herbaceous and sparse vegetation	C		Kasischke & Bourgeau-Chavez,1997
Low density marshes	C	VV	Pope et al., 1997
High density marshes	C	HH, VV	Pope et al., 1997
Non-woody and herbaceous wetlands	C	HH,VV	Kasischke & Bourgeau-Chavez, 1997

With regard to incidence angle of the radar beam, the results vary inconsistently with forest type, stand structure, moisture content, and canopy. Steep incident angle multi-polarized data can be used to identify emergent and forested wetlands (Hess et al., 1990; Augusteijn and Warrender, 1998; Wang et al., 1995; Bourgeau-Chavez et al., 2001). Steep incidence angles are able to penetrate forest canopy cover best with L-band, however, multiple angles are preferred to discriminate between forest structures (Ramsey, 1998; Henderson & Lewis, 2008). Lower incidence angles for C-, X- and K-bands have been used to detect forested wetlands under leaf-off conditions (Ramsey, 1998; Henderson & Lewis, 2008).

A number of studies recommend using multi-temporal, multi-incidence angle combinations to detect wetlands (Kandus et al., 2001; Leconte & Pultz 1991; Henderson & Lewis, 2008). However, Wang et al. (1998) in their land cover study including cattails, *Phragmites* (common reed) and tree covered swamp wetlands using ERS imagery data, found that adding multiple date images increased accuracy, only up to a certain point, where more than 5 images decreased accuracy. Grings et al. (2006) found that multi-temporal, multi-polarized C-band data can be used to accurately monitor temporal changes of marsh grasses, specifically within junco (cylindrical) and cortadera (randomly oriented disc) marshes. They found large differences in HH and VV backscatter from junco marshes, specifically, a change in the HH/VV ratio response. The VV data were also found to have increased sensitivity to plant density (Grings et al., 2006).

Polarimetric SAR systems transmit and receive waves in the horizontal and vertical polarizations. The system records the amplitude and relative phase in all four polarization combinations (HH, HV, VH, and VV). The received backscatter data are stored in scattering matrix S. From the scattering matrix, polarimetric data can be expressed into useful parameters such as the co-polarized phase difference. Such data allows also representing the scattering power graphically through polarization signatures. Co-polarized polarimetric signatures allow defining another polarimetric parameter, the pedestal height. Finally, polarimetric data allow expressing the scattering mechanisms through incoherent target decompositions. These polarimetric variables and decomposition can be useful in image classification.

Optical sensors such as Landsat's Multispectral Scanner System (MSS), Thematic Mapper (TM) and SPOTs High Resolution Visible (HRV) imaging have been used in wetland mapping. (Li & Chen, 2005). However, due to limitations in optic sensors, they cannot

penetrate vegetation canopies, which pose a problem in dense vegetation wetlands. The combination of radar and optical sensors is a promising approach, as together they provide complementary information (Ramsey et al., 2009).

Li & Chen (2005) used rule-based decision tree, to classify wetlands in three different study sites in Canada using Landsat, Radarsat-1 C-band and Digital Elevation Model (DEM) data. Wetland classification improved using a rule based approach where they analyzed multi-source data individually, then combined the results in a separate joint analysis. From this, they were able to distinguish between different wetland types and overall classification of rule-based method was 83% compared to 69% using classical supervised classification.

Some limitations existed for C-band radar, as it could not penetrate dense canopy forests (Li & Chen, 2005). Slight classification improvement of wet areas in agricultural landscape in Spain was found when using SAR ERS-2 and Landsat together than separately (Castañeda & Ducrot, 2009). Michelson et al. (2000) compared ERS-1 SAR data to the combination of Landsat and ERS -1 SAR for Swedish land cover, and found better separation in land cover classes with the combination than with SAR alone.

1.4. Classification methods

Classification and interpretation of SAR data are more complex than other multispectral imagery. Maximum likelihood classifiers are one of the most widely used in remote sensing. It operates by assigning a pixel to the class whose likelihood is the highest. This method is standard and simplistic, and assumes equal probability of class occurring, as it is not given use information about class occurrence frequency. By assuming equal probability, maximum likelihood may over-classify less frequent classes, and under-classify others (Pedroni, 2003). Maximum likelihood classifiers have been used in many studies, however, due to the complex nature of SAR images it may not be the optimal choice. For example, it assumes a Gaussian distribution of the data, while polarimetric SAR data have been shown to follow a Wishart distribution (Lee et al., 1994).

In order to accommodate the difference in the data distribution of multi-look polSAR data, such as filtered polSAR images (Wishart) (Lee et al., 1994) and of optical data (Gaussian), it is desirable to use a non-parametric classifier. Indeed, such classifier does not involve estimation of statistical parameters before classification and thus has its performance independent of the probability distribution functions of the input data. One of these classifiers is the Random Forests classifier. It is an ensemble classification method where multiple classifications are performed and their results combined through a voting process.

Random Forests is a tree type classifier that uses bootstrap aggregating to generate training sample subsets (Gislason et al., 2006; Waske and Braun, 2009). Each training sample subset is used to create an individual decision tree which is applied to produce an independent classification. When the independent classifications are run, they are then combined into the final classification map (Waske and Braun 2009). Random Forests are not sensitive to noise or over classifying, and can estimate the importance of the individual input variables (Gislason et al., 2006; Waske and Braun 2009). Waske and Braun (2009) compared boosting, Random Forest, Gaussian maximum likelihood and decision tree classifying methods for general landscape classification of SAR images. They found that Random Forests classifier outperformed decision tree and maximum likelihood classifiers.

1.5 Objectives

The purpose of this thesis is to determine the potential for using multi-beam Radarsat-2 C-band polarimetric SAR imagery for classifying wetland and non-wetland classes in a forested watershed. In particular, the influence of different factors on classification of SAR data were to be investigated, namely the sensor properties, the environmental conditions, the classification method, the addition of optical data and DEM-derived slope information, and the use of polarimetric variables. Specifically, the individual objectives were to:

1. Determine the influence of some environmental conditions and sensor properties for classification of forested and open wetlands using SAR images, and their seperability from other classes. Factors under examination were:

    i. Leaf-on vs. leaf-off,
    ii. Wetness conditions (using two classes: “dry” and “wet”),
    iii. Radar beam incidence angle (using two classes: 22° and 41-46°),
    iv. Single polarization (HH) vs. multi-polarization (HH, HV, and VV),

2. Determine if classification results improved with the combination of SAR, Landsat and DEM-derived slope data.

3. Test two different types of classifiers, namely maximum likelihood classification (MLC) and Random Forests (RF).

4. Test the use of polarimetric SAR images for classification and determine which polarimetric variables are the most useful.

2. Study Area

The study area is a 15 km x 17 km area within the Turkey Lake watershed and surrounding area in Ontario, Canada (Figure 2). It is located approximately 50 km north of Sault Ste. Marie, between 47°02’ and 47°05’ North, and 84°23’ and 84°27’ West. The landscape consists of mostly mixed hardwood forests. As indicated by the 1:50,000 DEM, the elevation differential is 290 m, ranging from 340 m above sea level at the lower streams to 630 m above sea level at the highest point on “*Batchawana Mountain*”. The drainage network is composed of five lakes, the largest being *Big Turkey Lake*. The overall discharge direction of lakes is from Upper and Lower *Batchawana Lake* to *Wishart Lake* to *Little and Big Turkey Lake* then flowing from *Norberg Creek* into *Batchawana River*.

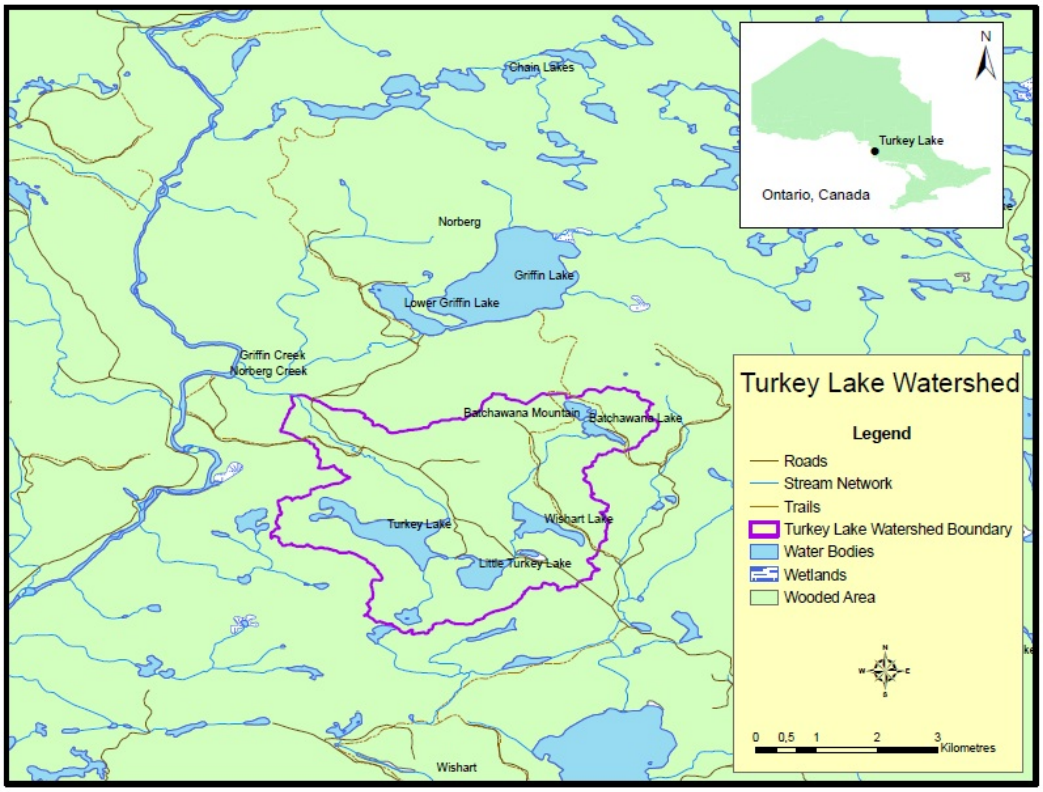

Figure 2. Map of Turkey Lake watershed and surrounding area.

Eight land cover classes were used in this study: hardwood forest, softwood forest, open wetland, closed wetland, harvest areas, low vegetation, bare soil, and water (Figure 3). The hardwood and softwood forest classes are non-wetland forest classes. Hardwood forest is dominated by deciduous trees. In this area the predominant deciduous tree species is sugar maple (*Acer saccharum*). The softwood forest class consisted of white pine (*Pinus strobes*), white spruce (*Picea glauca*) and eastern white cedar (*Thuja occidentalis* mix.). Wetland classes were separated into open wetland, which consists of both fens and marshes, and closed wetland which consisted of forested swamps where the predominant tree cover was deciduous. Harvest areas consist of recent clear cuts. Low vegetation was dry areas with short bushes and shrubs.

Closed Wetland – Hardwood swamp

Open Wetland – Fen

Hardwood Stand

Softwood Stand

Harvest Area

Figure 3. Ground photographs of some of the land cover types.

3. Materials and Methods

3.1 Imagery

In this study two types of satellite imagery for wetland mapping were used: (1) Radarsat-2 Single Look Complex (SLC) Fine Quad polarization (FQ) polarimetric SAR (pixel size that varies with the beam mode (Table 4), swath of 25 km), and (2) Landsat-5 TM optical (pixel size of 30 m, swath of 185 km) imagery. Fourteen Radarsat-2 SAR images (hereafter called "*FQ images*") were acquired in October-November 2010 and from May to November 2011 at different incidence angles, but with the same orbit descending pass (west-looking direction) (Table 4). These images were acquired under different leaf-off / leaf-on conditions, and different moisture conditions as shown by the precipitation data recorded at the Sault Ste. Marie weather station, approximately 62 km south of the study area (Table 4).

The Landsat-5 TM image was obtained from the USGS Landsat archive (glovis.usgs.gov). The image was acquired on May 17, 2010 leaf-on and was cloud, ice, and snow free. Five Landsat optical bands were used in the classification process. The bands used were TM 2 (0.52-0.60 µm, green), TM 3 (0.63-0.69 µm, red), TM 4 (0.76-0.90 µm, near-infrared), TM 5 (1.55-1.75 µm, short-wave infrared), and TM 7 (2.08-2.35 µm, short-wave infrared). TM 1 (the blue wavelength) was not used due to the potential atmospheric effects on the blue band.

A DEM (scale 1:50000) was obtained from Natural Resource Canada GeoGratis GeoBase archive (www.geogratis.gc.ca). The DEM had pixel spacing of 23 m × 17 m was used to georeference the SAR images, as they were not pre-processed when acquired. It was also used to create a slope dataset of the area, which was used in classification.

Table 4. Characteristics of the RADARSAT-2 polarimetric SAR images used for this study

Date	Beam Mode	Incidence Angle (degrees from nadir)		Pixel Spacing	Nominal Resolution (m)		Leaf conditions	Total precipitation (mm)*	Local time
		Near Range	Far Range	Range× Azimuth (m×m)	Near range	Far range			
27/10/2010	FQ 27	45.27	46.52	4.7 × 4.9	7.3	7.2	Leaf off	49	11:39
20/11/2010	FQ 27	45.27	46.52	4.7 × 4.9	7.3	7.2	Leaf off	0	11:39
20/05/2011	FQ 4	22.62	24.17	4.7 × 4.9	13.8	12.7	Leaf off	1.2	11:59
13/06/2011	FQ 4	22.27	24.17	4.7 × 4.9	13.8	12.7	Leaf on	24	11:59
24/06/2011	FQ 27	45.28	46.53	4.7 × 4.9	7.3	7.2	Leaf on	45.4	11:39
07/07/2011	FQ 4	22.26	24.17	4.7 × 4.9	13.8	12.7	Leaf on	12.2	11:59
11/07/2011	FQ 22	41.10	42.47	4.7 × 5.5	7.9	7.7	Leaf on	34.6	11:43
04/08/2011	FQ 22	41.10	42.48	4.7 × 5.5	7.9	7.7	Leaf on	6.6	11:43
24/08/2011	FQ 4	22.26	24.17	4.7 × 4.9	13.8	12.7	Leaf on	7.6	11:59
28/08/2011	FQ 22	41.09	42.48	4.7 × 5.5	7.9	7.7	Leaf on	2.4	11:43
17/09/2011	FQ 4	22.25	24.16	4.7 × 4.9	13.8	12.7	Leaf on	3.8	11:59
11/10/2011	FQ 4	22.25	24.16	4.7 × 4.9	13.8	12.7	Leaf off	0	11:59
15/10/2011	FQ22	41.09	42.47	4.7 × 5.5	7.9	7.7	Leaf off	48.2	11:43
08/11/2011	FQ 22	41.09	42.47	4.7 × 5.5	7.9	7.7	Leaf off	4.6	11:43

(*) mm of rain 3 days prior the image acquisition date that were recorded at Sault Ste. Marie weather station, approximately 62 km south of the study area

3.2 Training Data

Training areas were delineated for the following classes were 1) Hardwood forest, 2) softwood forest, 3) closed wetland (forested wetland or swamp), 4) open wetland (Fens), 5) harvest area, 6) low vegetation (grasses), 7) bare soil and 8) water (Figure 4). They were based on GPS ground-truth points that were collected in August 2011 and visual interpretation of the Landsat-5 TM images. Table 5 shows the number of polygons used in the classification, as well as total area of each class.

Table 5. Training data polygons used in classification

Class	**Number of Polygons**	**Total Area (ha)**
Hardwood Forest	23	55.1
Softwood Forest	34	62.9
Closed Wetlands	15	29.8
Open Wetlands	38	22.5
Harvest Area	16	20.4
Low Vegetation	7	24.7
Bare Soil	6	7.7
Water	10	219.7
Total	**149**	**442.8**

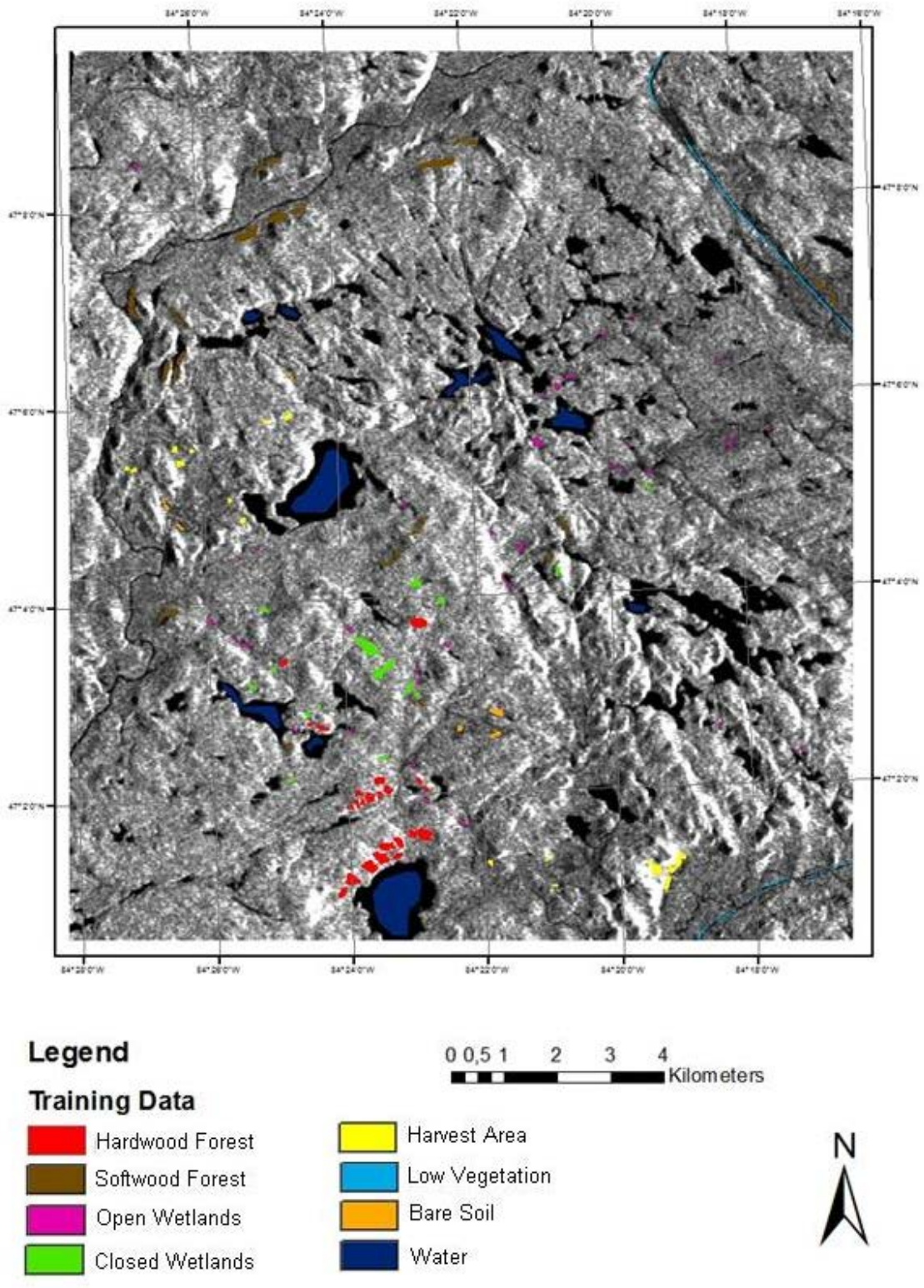

Figure 4. Radarsat-2 FQ 22 C-HV image with the whole set of training areas used in the classification.

3.3 Pre-classification processing of the FQ images

The FQ images had to undergo pre-classification processing. All the processing was completed using *PCI Geomatica* software. The raw image was extracted, then a Gaussian filter with 11×11 pixels window size was used to reduce speckle. Speckle is an inherent characteristic property of SAR imagery, generated by the phase interference of coherent signals from various scattering surfaces within a pixel, and imparts granularity to a SAR image (Goodman, 1976). The resultant combination of signals can either reduce or amplify the intensity of return, resulting in darker or brighter pixels. The application of a filter can reduce this effect (Lillesand et al., 2008).

The polarimetric analysis of the FQ images uses the full polarimetric information of the images that includes also the phase information. All the polarimetric analysis was performed using the *SAR Polarimetric Work Station (SPW)* module of *PCI Geomatica*. Speckle noise was removed by applying a 5×5 polarimetric Lee speckle filter (Lee et al., 1999). This filter preserves polarimetric properties by filtering each element of the covariance matrix independently, while maintaining spatial information. Various polarimetric product images were produced that include the co-polarized phase difference, the co-polarized correlation coefficient, and the pedestal height. Incoherent target decomposition techniques were also applied to produce the variables that are listed in Table 6.

Table 6. Incoherent target decompositions used in study

Decompositions	**Variables**
Cloude-Pottier	Alpha, Anisotropy, Entropy, Beta
Freeman-Durden	Power contributions due to double-bounce, volume scattering, and rough surface.
Touzi	Psi Angle, Dominant Eigenvalue, Touzi Alpha_S Parameter, Phase
Van Zyl	Van Zyl classes

Both the multi-polarized and polarimetric FQ images were then orthorectified using the *"Radarsat-2 Rational Function Model"* function of the *Orthoengine* module of *PCI Geomatica*. It used DEM and Ground Control Points (GCP), which were extracted from the Landsat-5 TM georeferenced images. Accuracy of the orthorectification process and number of GCPs used are recorded in Table 7. The Landsat-5 TM image pixels were split into 3×3 10m pixels to match the 10 m spacing of the FQ images. The resulting FQ images have a 10 m resolution and a UTM Zone 16T122D projection with a NAD83 datum.

Table 7. Orthorectification accuracy

Image Date	Number of Ground Control Points	RMS Error(*)		
		X	Y	Mean
27/10/2010	25	1.43	1.73	2.25
20/11/2010	25	2.22	1.37	2.61
20/5/2011	25	2.03	1.63	2.60
13/06/2011	25	2.19	1.87	2.88
24/06/2011	25	1.88	1.44	2.37
07/07/2011	27	2.22	1.89	2.91
11/07/2011	25	2.33	1.51	2.78
04/08/2011	26	2.29	1.49	2.73
24/08/2011	25	2.65	2.45	3.61
28/08/2011	25	1.97	1.81	2.68
17/09/2011	25	2.58	2.08	3.31
11/10/2011	25	2.27	1.87	2.94
15/10/2011	26	2.34	1.73	2.91
08/11/2011	25	1.84	1.89	2.64

*Root Mean Square (RMS) errors are given in pixels

3.4 Classification

The filtered and orthorectified images were then used in a Maximum Likelihood Classification (MLC) and Random Forests classification. MLC assumes a Gaussian (normal) distribution and evaluates both the variance and covariance of a class when classifying an unknown pixel. The statistical probability of pixel being included in a class and the probability density function is calculated. MLC uses the Bayesian discriminant analysis to then determine which class is most "likely". The MLC classifier was tested using various FQ image combinations as a function of the polarization and the beam mode. From the polarization point of view, the following image combinations were used as image inputs into the MLC classifier:

i) HH: Representing the case of Radarsat-1 SAR images,
ii) HH, HV, and VV: Representing the case of multi-polarized Radarsat-2 SAR images.

The polarimetric variables were not used in the MLC classifier as they do not follow a Gaussian distribution that is assumed when using a MLC.

The FQ images were separated into seven different groups of two images each, based on rainfall, incidence angle, and leaf presence (Table 8). The images were sorted in this manner to help determine the effect that these different characteristics had on the classification of the radar images. Two images of each were used together for each classification to improve classification accuracy (Wang et al., 1998), and to have the same number of images in each grouping. The FQ images were considered as being acquired under wet conditions if the total rainfall amount over the three days prior the image acquisition date was greater than 10 mm. Conversely, the images were and considered as

being acquired under dry conditions, if this rainfall amount was less than 10 mm. For the beam mode, we consider in one hand, the steep incidence angle (22-24°) images (FQ4) and the other hand, the shallow incidence angle images (FQ22 & FQ27). We did not do a difference between the FQ22 and FQ27 images, because both have similar incidence angles. Indeed, FQ22 images were acquired under an incidence angle of 41-42° and FQ27 images are acquired under an incidence angle of 45-46° (Table 1). To determine if the FQ images were acquired under leaf-on or leaf-off conditions, the Landsat images matching the date of the FQ images were inspected visually. Unfortunately, there were no FQ4 images taken during leaf off and wet conditions.

Table 8. FQ image pairs used in the MLC classification

Leaf Presence	**Moisture Conditions**	**Rainfall (mm)**	**Beam Mode**	**Date**
Leaf-off	Dry	4.6	FQ 22	08/11/2011
		0	FQ 27	20/11/2010
		1.2	FQ 4	20/05/2011
		0	FQ 4	11/10/2011
Leaf-on	Dry	6.6	FQ 22	04/08/2011
		2.4	FQ 22	28/08/2011
		7.6	FQ 4	24/08/2011
		3.8	FQ 4	17/09/2011
Leaf-on	Wet	45.4	FQ 27	24/06/2011
		34.6	FQ 22	11/07/2011
		24	FQ 4	13/06/2011
		12.2	FQ 4	07/07/2011
Leaf-off	Wet	49	FQ 27	27/10/2010
		48.2	FQ 22	15/10/2011

After classification of the FQ data alone, for the FQ image pair that gave the highest classification accuracy, the classifier was run using a combination of the FQ image pair and the Landsat image (May 2010). In a next step, DEM-derived slope was added to the FQ/Landsat combination, as slope can be a useful tool in delineating wetland presence. In addition, classification of the single Landsat image was also performed in order to make a comparison.

Random Forests uses a combination of decision trees classifiers that uses bootstrap aggregating to generate training sample subsets in individual classification, which are then in turn used in a final classification result. The Random Forests classifier was performed using the Random Forests algorithm in R (R Development Core Team, 2012). Classification using Random Forests was completed using the FQ image pair giving the best MLC cross-validation overall accuracy (leaf-off, dry, FQ22/27), alone, and in combinations with the Landsat data and slope. For each classification, the settings used were 800 trees. The *m*try variable was set to include all input features.

Random Forests can be used to select the input features that are able to best separate between classes, called “variable importance”. Random Forests was therefore run using all 14 FQ images and polarizations (HH, HV, VH, and VV) creating a 56 band file, to see

which bands were found most important or useful. It was also run using the polarimetric variables of Table 6 for the leaf-off dry, FQ22/27 image pair. This was done in attempt to see if the polarimetric variables provided a better classification than just the HH, HV, VV intensity images alone, and to see which polarimetric variables provided the most useful information. In the case of the polarimetric classification, the *m*try was set to 15 (out of 39).

Theoretically, classification accuracy should be assessed against existing independent data, for example, from field work, aerial photo interpretation, or detailed land cover maps. However, as noted previously, this was not possible due to the lack of these types of data over the area. Hence, for this study, the performance of the different classification algorithms and the effect of the input data were compared using cross-validation. The cross-validation results are expressed in error matrices, showing Producer's individual class accuracies, and corresponding average accuracies, overall accuracies and Kappa coefficients. The Producer's class accuracy for class *i* is the number of pixels that are labeled as class *i* in both the classified and ground-truth images divided by the total number of pixels of class *i* in the ground-truth image (Congalton, 1991). The corresponding average accuracy is the simple average of individual class accuracies, whereas the corresponding overall accuracy is the average of individual class accuracies, weighted by the size of class samples for that class in the total training set. The Kappa coefficient can be interpreted like a coefficient of correlation, with values close to 0 indicating poor classification accuracies and values closer to 1 indicating good classification accuracies.

4. Results

4.1 Maximum likelihood classification

The cross-validation results for the various FQ images classified using the MLC are shown in Table 9. The FQ image pair that gave the best overall result (76.3%) using the MLC was the FQ22-27 images acquired under leaf-off and dry conditions (Table 9). The corresponding confusion matrix shows that for the non-water classes, the user's accuracy is the highest for the softwood (67.0%) and low vegetation (69.4%) classes, but the lowest for the open wetlands class (26.6%) (Table 10).

Table 11 presents the cross-validation for results from classifying the Landsat-5 TM image alone and for the leaf-off, dry, FQ 22/27 images combined with Landsat-5 TM and/or slope data. Adding five optical bands from the Landsat-5 TM image in the classification process for the FQ22-27 images acquired under leaf-off and dry conditions increased the cross-validation result for the individual classes. The overall accuracy increased from 73.3% to 94.4%. The addition of the slope data to the classification only slightly increased the overall classification accuracy to 95.4%. The corresponding classified image is presented in Figure 5 and the corresponding confusion matrix is presented in Table 12. For the non-water classes, the user's accuracy is the highest for the forested classes (hardwood class with 99.4% and softwood class with 91.5%) as well as for the low vegetation class (91.4%). The open wetlands class has a user's accuracy that increased from 26.6% to 80.5% (Table 12).

Table 9. Cross-validation results (%) for the MLC applied to various combinations (*) of multi-polarized Radarsat-2 SAR images as a function of the beam mode, polarization and acquisition condition

Conditions	Beam Mode	Bands or Polarization	Hardwood Forest	Softwood Forest	Closed Wetland	Open Wetland	Harvest Area	Low Vegetation	Bare Soil	Water	Average Accuracy	Overall Accuracy	Kappa coefficient
Leaf-off, Dry	**FQ 22/27**	HH	29.4	61.6	47.3	18.2	28.5	21.3	32.8	99.5	42.3	69.0	56.1
		HH,HV,VV	**53.8**	**67.0**	**59.4**	**26.6**	**40.4**	**69.4**	**61.2**	**96.6**	**59.3**	**76.3**	**66.9**
	FQ 4	HH	16.0	76.1	61.4	3.2	43.2	35.5	61.9	92.4	48.7	68.0	55.5
		HH,HV,VV	36.4	81.1	64.4	16.3	56.5	58.5	58.9	90.0	57.8	72.8	62.6
Leaf-on, Dry	FQ 22/27	HH	20.6	71.6	43.5	11.2	37.2	3.6	54.2	99.6	42.7	68.5	55.4
		HH,HV,VV	29.2	75.9	56.6	15.2	42.6	27.9	58.4	97.6	50.4	72.0	60.6
	FQ 4	HH	21.9	58.6	45.3	0.0	47.1	31.6	44.3	91.2	42.5	64.0	49.2
		HH,HV, VV	27.6	82.3	65.1	8.3	53.7	51.8	50.4	93.2	54.1	72.4	61.9
Leaf-on, Wet	FQ 22/27	HH	22.7	71.9	46.5	19.2	30.6	12.7	30.2	99.5	41.7	69.2	56.3
		HH,HV,VV	29.5	77.9	50.4	20.1	35.0	30.0	53.5	98.4	49.3	72.2	60.8
	FQ 4	HH	24.3	78.0	62.8	17.0	40.3	4.8	52.3	94.7	46.8	69.2	56.7
		HH,HV,VV	23.7	82.1	59.8	19.4	51.2	35.0	60.2	92.5	53.0	70.9	59.7
Leaf-off, Wet	FQ 22/27	HH	31.5	67.0	62.1	27.3	30.4	12.3	39.4	98.6	46.1	70.7	58.6
		HH,HV,VV	56.8	73.5	57.9	33.6	47.2	43.8	56.3	94.5	57.9	75.6	66.0

(*) the best FQ pair is highlighted in bold

Table 10. Confusion matrix for the best case from MLC which was the Radarsat-2 HH, HV and VV FQ22/27 leaf-off, dry image pair

Class	**Hardwood Forest**	**Softwood Forest**	**Closed Wetland**	**Open Wetland**	**Harvest Area**	**Low Vegetation**	**Bare Soil**	**Water**	**Total**	**User's Accuracy**
Hardwood Forest	2962	144	1487	24	867	0	24	0	5508	53.8
Softwood Forest	180	4215	683	385	64	440	231	93	6291	67.0
Closed Wetland	259	363	1775	144	233	23	178	0	2975	59.7
Open Wetland	50	318	166	599	150	770	197	0	2250	26.6
Harvest Area	301	152	472	108	824	18	167	0	2042	40.4
Low Vegetation	12	146	40	186	138	1715	235	0	2472	69.4
Bare Soil	3	29	41	76	59	89	469	0	766	61.2
Water	5	43	1	3	33	665	4	21218	21972	96.6
Total	3772	5410	4665	1525	2368	3720	1505	21311	44276	
Producer's Accuracy	78.5	77.9	38.1	39.3	34.8	46.1	31.2	99.6		76.3

Table 11. Cross-validation results (%)for the MLC applied to Landsat-5 TM alone and to the multi-polarized FQ 22/27 leaf-off dry image pairs (*) combined with Landsat-5 TM and/or slope derived from the DEM. All the images were acquired under dry conditions. The best case is highlighted in bold

Conditions	**Sensor (and Beam Mode)**	**Bands or Polarizations**	**Hardwood Forest**	**Soft-wood Forest**	**Closed Wetland**	**Open Wetland**	**Harvest Area**	**Low Vegetation**	**Bare Soil**	**Water**	**Average Accuracy**	**Overall Accuracy**	**Kappa Coefficient (%)**
Leaf-on,	Landsat -5 TM	TM 2,3,4,5,7	96.2	81.2	85.1	75.8	88.4	77.0	96.6	99.7	87.5	92.6	89.6
Leaf-off, Dry	FQ 22/27 and Landsat-5	HH, HV,VV, TM 2-7	99.5	87.3	86.6	76.8	90.4	84.6	96.7	99.5	90.2	94.4	92.1
Leaf off, Dry	FQ 22/27 and Slope	HH, HV, VV, Slope	65.6	79.0	64.9	44.6	48.0	67.4	59.1	96.1	65.6	80.7	73.1
Leaf-off, Dry	**FQ 22/27 and Landsat-5 TM and Slope**	**HH, HV,VV, TM 2-7, Slopes**	**99.4**	**91.5**	**88.1**	**80.5**	**91.4**	**85.9**	**96.6**	**99.4**	**91.6**	**95.4**	**93.5**

(*) the best FQ pair from the initial MLC result

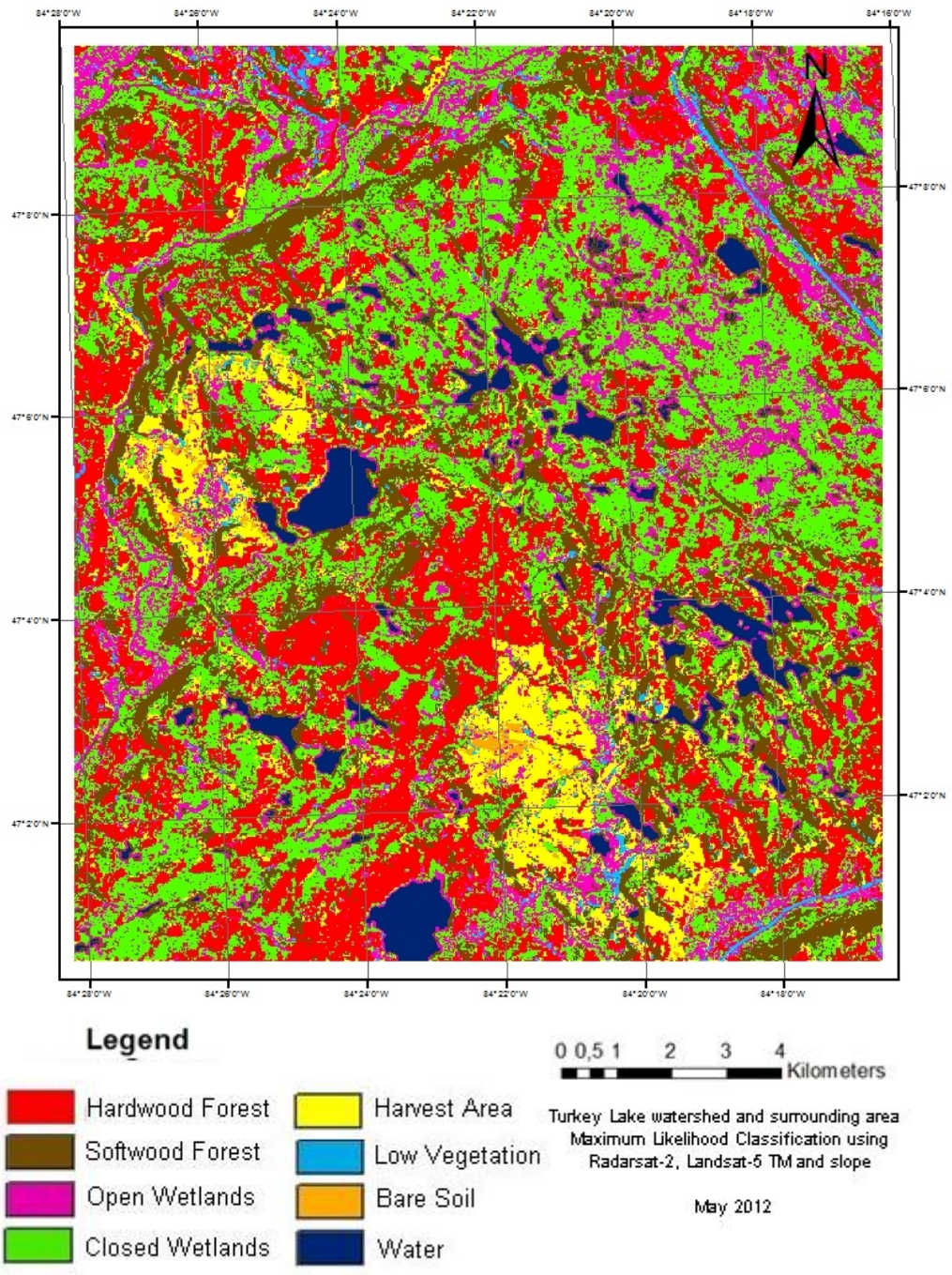

Figure 5. Classified image of the Turkey Lake watershed area obtained by applying a MLC to a combination of Radarsat-2 (HH, HV, VV) FQ 22/27 images which were acquired under leaf-off, dry conditions, Landsat -5 TM (TM bands 2, 3, 4, 5 and 7), and slope data.

Table 12. Confusion matrix for the MLC applied to the Radarsat-2 (HH, HV, and VV) FQ 22/27 image pair combined with the Landsat -5 TM (TM bands 2, 3, 4, 5 and 7) image and slope data

Class	Hardwood Forest	Softwood Forest	Closed Wetland	Open Wetland	Harvest Area	Low Vegetation	Bare soil	Water	Total	User's Accuracy
Hardwood Forest	5477	4	6	16	2	3	0	0	5508	99.4
Softwood Forest	8	5754	337	164	27	1	0	0	6291	91.5
Closed Wetland	18	185	2620	145	6	1	0	0	2975	88.1
Open Wetland	20	33	107	1811	25	215	39	0	2250	80.5
Harvest Area	9	0	0	40	1867	18	108	0	2042	91.4
Low Vegetation	7	8	0	244	88	2124	1	0	2472	85.9
Bare Soil	0	0	0	4	22	0	740	0	766	96.6
Water	0	55	1	63	2	1	0	21850	21972	99.4
Total	5539	6039	3071	2487	2039	2363	888	21850	44276	
Producer's Accuracy	98.9	95.3	85.3	72.8	91.6	89.9	83.3	100.0		95.4

4.2 Random Forests

The cross-validation results from the Random Forests classifications are summarized in Table 13. The overall classification accuracy increased from 86.7% (when only the leaf-off dry FQ22/27 image pair was used) to 98.6% (when the Landsat optical images were added to the classification). Adding the slope resulted in only a very small improvement (overall accuracy of 98.7%). A similar overall accuracy (98.3%) is obtained when all the multi-polarized (HH, HV, VH, and VV) FQ images are used. The classified image resulting from the combined leaf-off, dry FQ22/27 image pair and Landsat -5 TM is shown in Figure 6. The classified image for leaf-off, dry FQ22/27, Landsat and the slope data are shown in Figure 7, and in Figure 8, the case where all the multi-polarized FQ images are used is shown.

Random Forests allows the identification of variable importance, indicating which input features were most important to achieving the highest accuracy for separating different classes. These features are presented in Figures 9, 10 and 11, giving the variable importance for the cases where the input was Radarsat-2 and Landsat-5 TM; Radarsat-2, Landsat-5 TM and slope; and, All radar images. The figures illustrate variable importance through mean decrease in accuracy, where the most important variables have the highest mean decrease accuracy. Mean decrease in accuracy is a measure of the accuracy decrease when another variable is added, thus a variable with a large decrease in accuracy would be more important. The variables are ordered by importance in Table 14 for the case when all the multi-polarized FQ images are used.

Table 13. Cross-validation results (%)for the Random Forests classifier applied to all multi-polarized FQ images, to the multi-polarized FQ 22/27 leaf-off dry image pair (*) alone or combined with Landsat-5 TM and/or slope data, and to polarimetric products that were computed for the FQ22 and FQ 27 leaf-off dry images

Images	**Hardwood Forest**	**Softwood Forest**	**Closed Wetland**	**Open Wetland**	**Harvest Area**	**Low Vegetation**	**Bare Soil**	**Water**	**Average accuracy**	**Overall accuracy**
All FQ images	99.0	98.6	93.6	90.4	95.5	97.9	97.0	99.8	96.5	98.3
Leaf-off, dry, FQ22/27	87.0	86.8	65.8	55.2	43.3	68.8	62.1	99.5	71.1	86.7
Leaf-off, dry, FQ22/27, and slope	91.0	92.6	82.1	67.6	53.6	74.8	72.3	99.8	79.2	90.8
Leaf-off, dry, FQ22/27, and Landsat-5 TM	99.8	97.4	95.9	92.6	98.0	95.9	98.2	100.0	97.2	98.6
Leaf-off, dry, FQ22/27, slope, and Landsat	99.8	98.0	96.2	93.6	97.7	96.0	97.4	100.0	97.3	98.7
Polarimetric variables of the FQ27 image	82.3	74.1	17.7	12.3	8.8	37.6	12.4	99.6	43.1	74.7
Polarimetric variables of the FQ22 image	79.5	74.3	23.8	17.6	11.0	46.7	19.1	99.6	46.4	75.8

(*) the best FQ pair from the initial MLC result

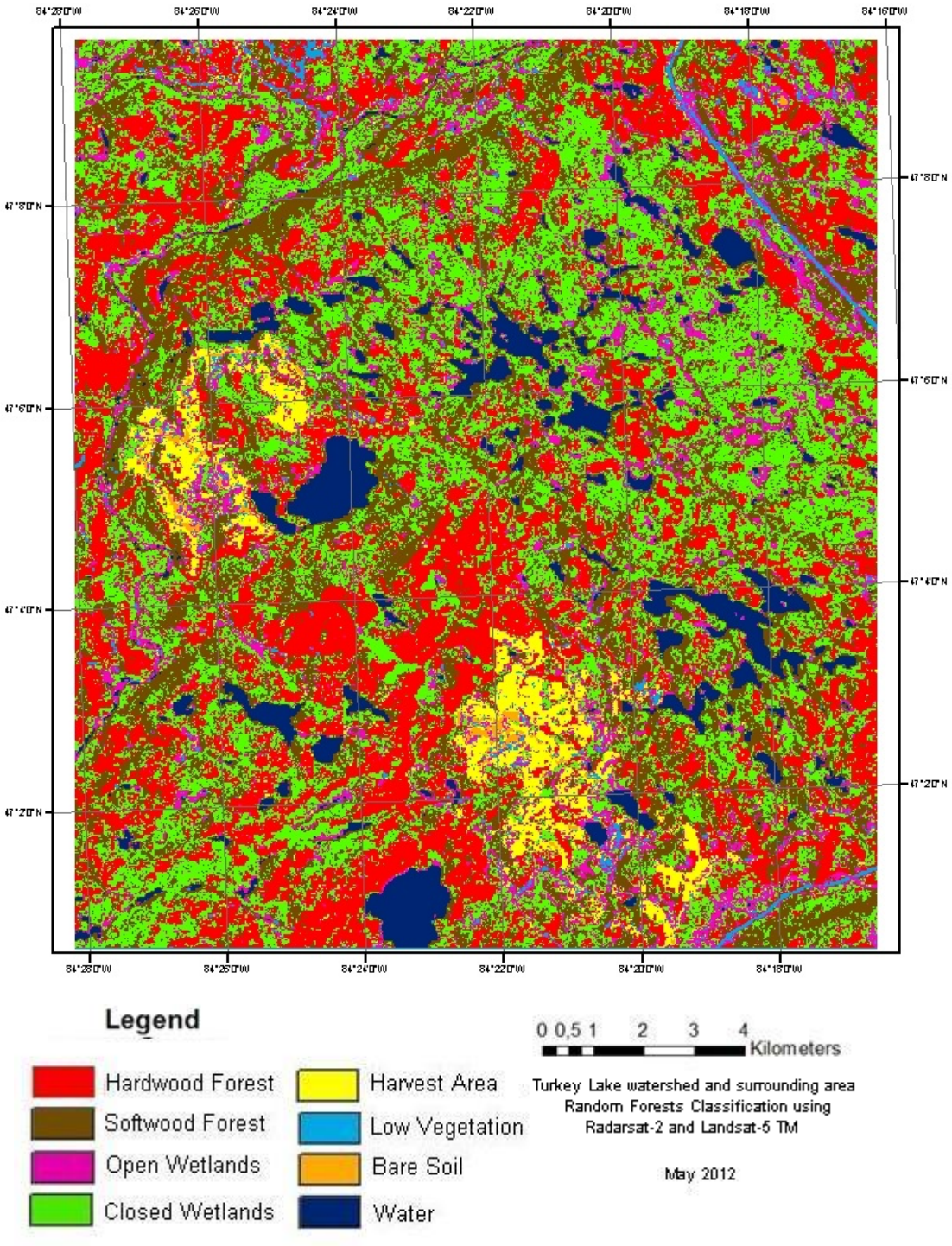

Figure 6. Classified image of the Turkey Lake watershed area obtained by applying Random Forests to a combination of Radarsat-2 (HH, HV, VV) FQ 22/27 image pair acquired under leaf-off and dry conditions plus Landsat-5 TM (TM bands 2, 3, 4, 5 and 7) data.

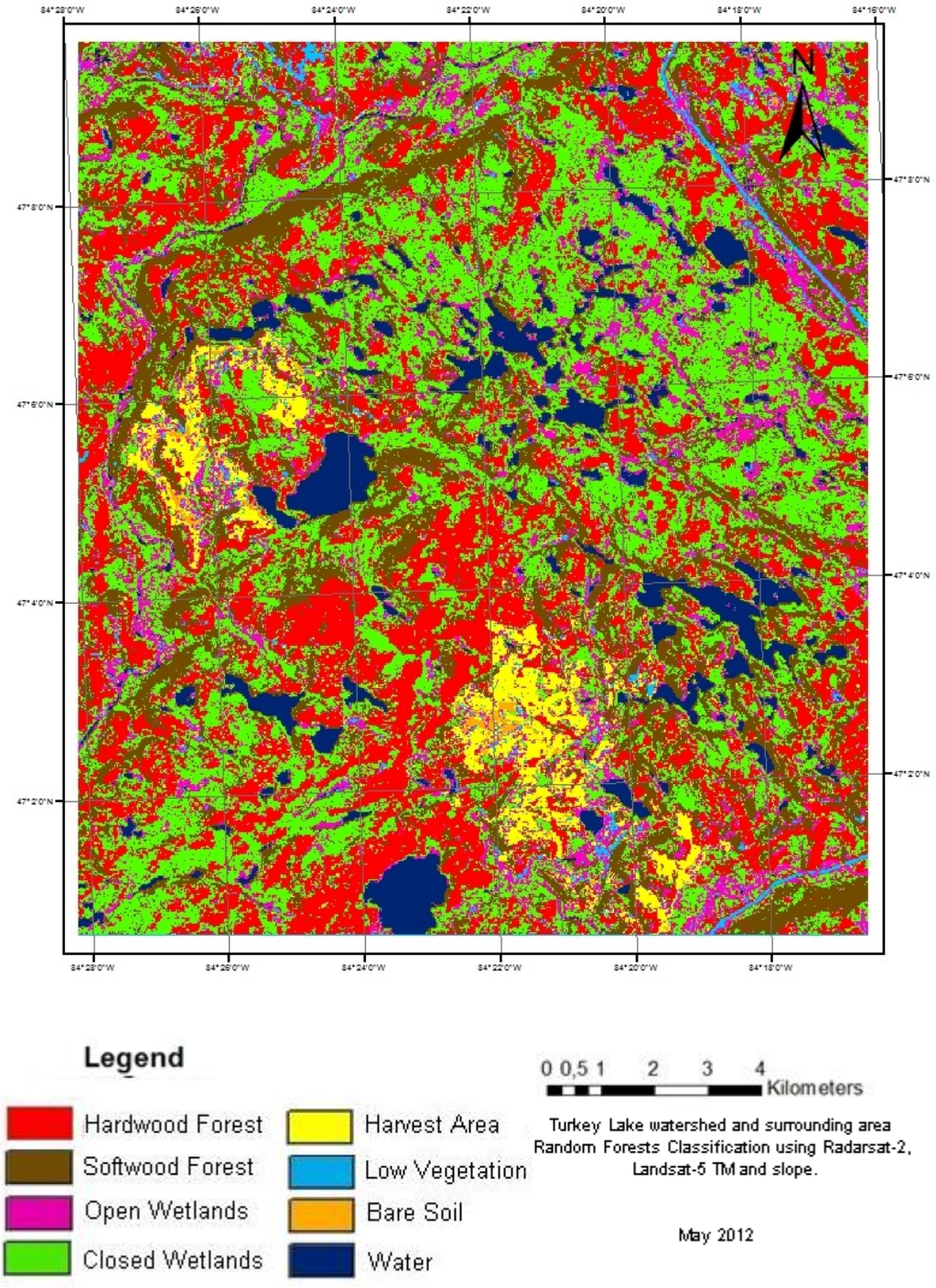

Figure 7. Classified image of the Turkey Lake watershed area obtained by applying Random Forests to a combination of Radarsat-2 (HH, HV, VV) FQ 22/27 image pair acquired under leaf-off and dry conditions, Landsat-5 TM (TM bands 2, 3, 4, 5 and 7), and slope data.

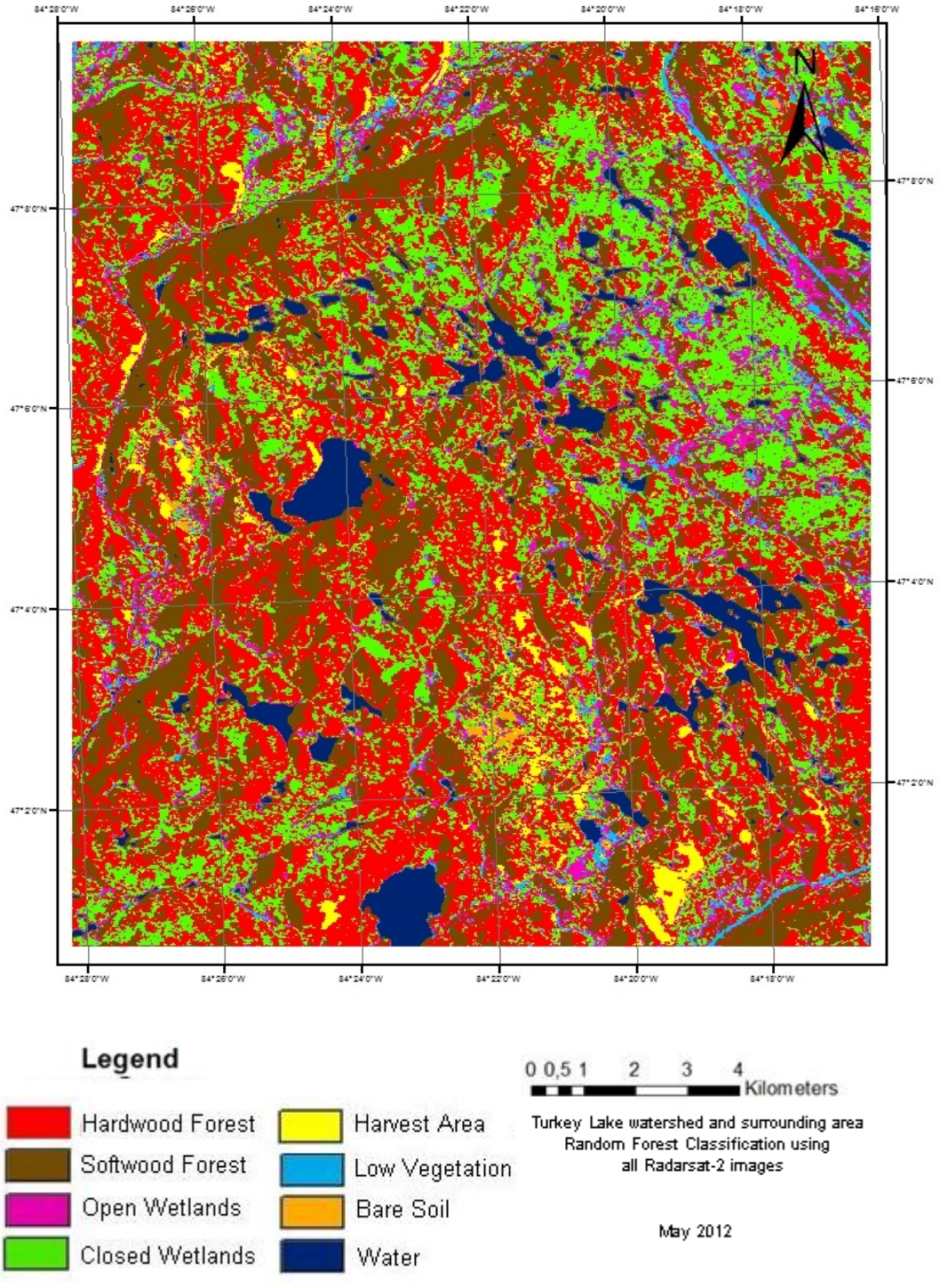

Figure 8. Classified image of the Turkey Lake watershed area obtained by applying Random Forests classification to all the multi-polarized FQ images (HH, HV, VH, VV).

Figure 9. Variable importance in terms of mean decrease in accuracy in Random Forests classification for the case when leaf-off dry FQ22/27 images and Landsat-5 TM are used. The image file name listed in the figure reads as follows: RS (for Radarsat-2), date and polarization, and b followed by a number represents the different Landsat TM bands.

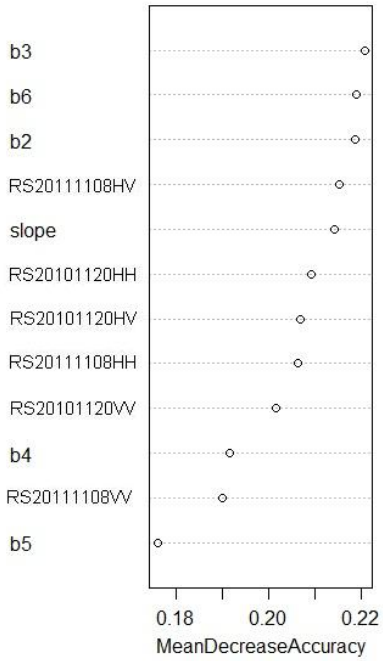

Figure 10. Variable importance in terms of mean decrease in accuracy in Random Forests classification for the case when leaf-off dry FQ22/27 images, Landsat-5 TM and slope are used. The image file name listed in the figure reads as follows: RS (for Radarsat-2), date and polarization, and b followed by a number represents the different Landsat TM bands.

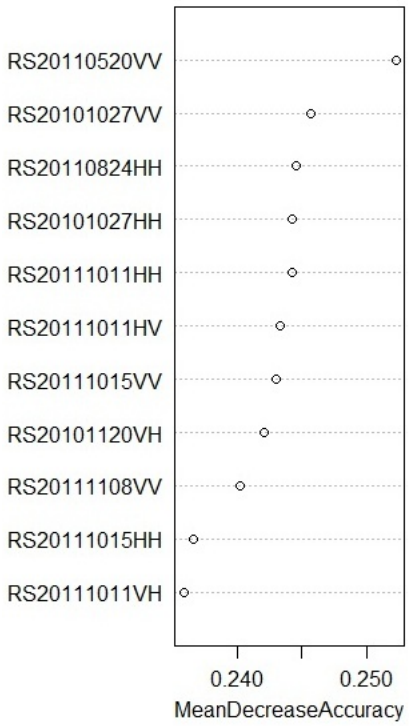

Figure 11. Variable importance in terms of mean decrease in accuracy in Random Forests classification for the case when all multi-polarized FQ images are used. The image file name listed in the figure reads as follows: RS (for Radarsat-2), date and polarization.

Table 14. Order of the variable importance from Random Forests for the case when all the multi-polarized FQ images are used

Order	Polarization	Image Date	Rain Fall (mm)	Moisture Conditions	Beam Mode	Leaf Presence
1	VV	20/05/2011	1.2	Dry	FQ 4	Leaf-off
2,4	VV, HH	27/10/2010	49	Wet	FQ 22/27	Leaf-off
3	HH	24/08/2011	7.6	Dry	FQ 4	Leaf-on
5,6,11	HH, HV, VH	11/10/2011	0	Dry	FQ 4	Leaf-off
7, 10	VV, HH	15/10/2011	48.2	Wet	FQ 22/27	Leaf-off
8	VH	20/11/2010	0	Dry	FQ 22/27	Leaf-off
9	VV	08/11/2011	4.6	Dry	FQ 22/27	Leaf-off

The classifications based on the polarimetric products computed with the leaf-off, dry FQ22 or FQ27 image gave the lowest cross-validation overall accuracies (74.73% and 75.82%, respectively). This is especially the case for the class accuracy associated to closed wetland, open wetland, and harvest areas (Table 13). When applying the variable importance of Random Forests to the polarimetric product-based classification, there are some polarimetric variables that were found to be the most useful in classification (Figure 12 for the FQ27 image and Figure 13 for the FQ22 image).

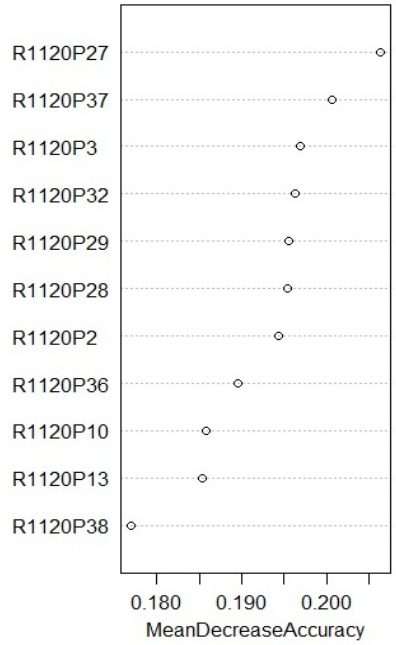

Legend:

Code	Polarimatric Variable
27	Freeman-Durden Volume Scattering
37	Touzi Alpha_S Parameter
3	Cloude-Pottier Beta Angle
32	LL Backscatter
29	PSI angle for minimum of the completely polarized component
28	PSI angle for maximum of the completely polarized component
2	Cloude-Pottier Anisotropy
36	Touzi Tau Angle
16	Maximum of the Scattered Intensity
13	Maximum of the completely unpolarized component
38	Touzi Phase

Figure 12. Variable importance in terms of mean decrease in accuracy in Random Forests classification for the polarimetric products of the leaf off, dry, FQ27 image of November 20, 2010. The image file name listed in the figure reads as follows: RS (for Radarsat-2), date and polarization code.

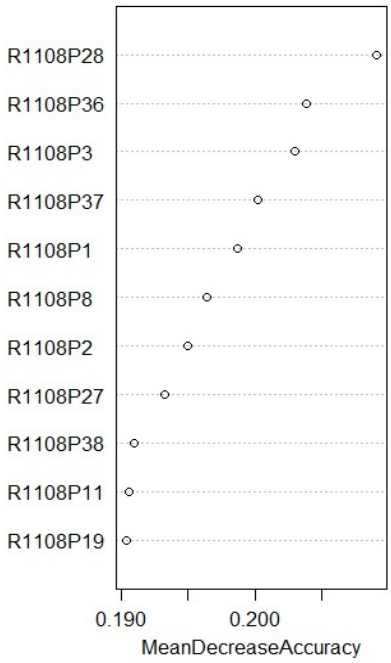

Legend:

Code	Polarimetric Variable
28	PSI angle for maximum of the completely polarized component
36	Touzi TauAngle
3	Cloude-Pottier Beta Angle
37	Touzi Alpha_S Parameter
1	Cloude-Pottier Alpha Angle
8	Cloude-Pottier Entropy
2	Cloude-Pottier Anisotropy
27	Freemand-Durden Volume Scattering
38	Touzi Phase
11	Magnitude of the correlation coefficient
19	Minimum of the degree of polarization

Figure 13. Variable importance in terms of mean decrease in accuracy in Random Forests classification for the polarimetric products of the leaf off, dry, FQ27 image of November 8, 2011. The image file name listed in the figure reads as follows: RS (for Radarsat-2), date and polarization code.

5. Discussion

In this study, the properties of Radarsat-2 polarimetric SAR images were investigated for their ability to distinguish between land cover types in a forested watershed. These classes included non-wetland forests, open wetlands, and closed (forested) wetlands. The influence of different factors on the classification of Radarsat-2 data were studied, namely different environmental factors and sensor characteristics, the classification method, the addition of optical satellite data and slope information, and the use of polarimetric variables. This study involved three data sources (Radarsat-2 polarimetric SAR, Landsat-5 TM, and slope derived from a DEM) and two different classification methods (Maximum Likelihood Classification and Random Forests).

5.1. Maximum Likelihood and Random Forests classification

For all classifications, Random Forests provided higher cross-validation overall accuracies than MLC (Table 14). Waske and Braun (2009) and Reese (2011) previously showed the superiority of Random Forests over the MLC for land cover mapping. In our case, SAR data is quite complex and polarimetric SAR data does not follow a Gaussian distribution which is an assumption for the MLC. Random Forests' ability to select the most important variables and weight their importance in the classification appears to be useful to classifying data.

Table 15. Comparison of overall accuracy between MLC and Random Forests Classification

Images	Overall Accuracy	
	MLC	Random Forests
Leaf-off dry FQ22/27 pair	76.3	86.7
Leaf-off dry FQ22/27 pair and Slope	80.7	90.8
Leaf-off dry FQ22/27 pair and Landsat TM2-7	94.4	98.6
Leaf-off dry FQ22/27 pair, Landsat TM2-7 and Slope	95.4	98.7

Since Random Forests is a non-parametric classifier, and does not require a normal distribution, it appears to classify the FQ data much better than the MLC (86.7% vs. 76.3%). However, the addition of Landsat and slope data to the FQ images in the classification appears to have a larger effect when using MLC than Random Forests, with an increase of 20% vs. 12%.

5.2 Radarsat-2 polarization, beam mode and environmental conditions

With the MLC method, the FQ images were classified by considering the HH polarization alone, and together with the HV and VV polarizations. For all the FQ images, using the three polarizations had a clear advantage over using HH alone. When applying a MLC multi-polarized Radarsat-2 FQ images for land cover mapping in a tundra environment, Shelat et al. (2012) also showed that considering three polarizations significantly improved the classification accuracy as compared to using only the HH polarization. When classifying all multi-polarized FQ images with Random Forests, the classifier selected VV and HH as the most important polarizations for the classification. Inclusion of Radarsat-2 C-VV polarized image in an MLC classifier was previously shown to facilitate differentiation between vegetated and non-vegetated areas in a tundra environment (Shelat et al., 2012). Other previous studies showed that the differences in backscatter between

flooded and non-flooded areas were the highest at HH and lowest at HV using SIR-C images acquired for the Red River flood in 1994 with an incidence angle of 39° (Crevier and Pultz, 1996; Sokol et al., 2004). This is due to the greater penetrating capability of the HH waves and the fact that the presence of water enhances the dominant scattering mechanism of the tree trunks in the HH polarization.

For MLC classification accuracies that were obtained using the FQ images alone, it appears that the most predominant factor influencing the classification is the season of image acquisition (leaf-on vs. leaf-off). All of the leaf-off images gave higher cross-validation results than the leaf-on images. A similar result is seen from the Random Forests variable importance analysis for the case when all the multi-polarized FQ images are used. Indeed, 10 of the top 11 most important input features correspond to the leaf-off images. This could be due to the fact that the radar beam does not have to penetrate through the leafy vegetation layer of the deciduous tree crowns and ground level vegetation, resulting in less signal/canopy interactions. This in turn allows easier access to ground information (including water of the wet areas) that makes it easier to distinguish between the *closed wetland* class versus the *hardwood* and *softwood forest* (Henderson & Lewis, 2008).

The incident angle seems to have some effects on the classification results. When using MLC, the FQ 22/27 beam modes (acquired at 41° - 46° incidence angle) performed better than the FQ 4 beam mode image (~22°) when they were acquired under leaf-off and dry conditions. However, when leaves are present, the FQ 4 beam mode performs better than the FQ 22/27 beam mode under dry conditions. The opposite occurs under wet conditions. The lowest classification accuracies were obtained with the FQ 4 pairs acquired over leaf-on and wet conditions (70.9%). From the Random Forests classification results, it appears that both the FQ modes were important in image classification, with FQ 4 images at the top of the list of variable importance. It is interesting to note that the only leaf-on image included as important was acquired with the FQ 4 incidence angle, indicating that maybe the lower incidence angle could penetrate the canopy easier than at the higher incidence angle. Shelat et al. (2012) classified land cover in a tundra environment with the MLC and multi-polarized RADARSAT-2 SAR images acquired in FQ1, FQ12 and FQ20. From this study they showed that moderate incidence angles (FQ12 or FQ20) performed better than steep incidence angles (FQ1).

The effect of moisture conditions based on the rainfall amount is less clear. This may be with due to identifying a threshold which defines what wet versus dry should be. As well, wetlands are generally wet without any rainfall, and therefore there shouldn’t be too much difference. With MLC, there is some indication that for leaf-off images, cross-validation resultswere better for images acquired under dry conditions than under wet conditions, whatever the beam mode. However, for the FQ 22/27 leaf-on images, the classification was slightly better when the image was acquired under wet conditions than under dry conditions. We cannot make any conclusions for the FQ 4 beam mode due to lack of leaf-on images acquired under wet conditions. From the Random Forests classification, both dry and wet images were considered to be important variables in classification.

5.3 Image combination of radar with optical data and slope

The MLC algorithm applied to the Landsat image alone gave a cross-validation overall result of 92.6%. For the FQ image pair, the highest cross-validation classification result (76.3%) was obtained with the FQ 22/27 image pair acquired under leaf-off and dry conditions. We can expect that using both the Landsat-5 TM and the FQ images will allow for better classification accuracy. When the Landsat-5 TM image was added to the FQ 22/27 image pair acquired under leaf-off and dry conditions, the MLC cross-validation result for overall accuracy increased to 94.4%. Further small improvement was made in the classification by adding slope data in the classifier, increasing the cross-validation result for overall accuracy to 95.4%. Adding Landsat-5 TM and DEM data to the MLC classification of SAR images had previously been shown to improve classification accuracy of surficial materials in tundra environment from Radarsat-1 C-HH SAR images (Grunsky et al., 2009), Radarsat-2 C-HH and C-HV images (LaRocque et al., 2012), and multi-polarized Radarsat-2 SAR images (Shelat et al., 2012). Indeed, different aspects of the land cover are captured by differences in spectral reflectance through the Landsat image, radar backscatter of the FQ images, and topography from the DEM, all of which help to differentiate the land cover classes.

The poorest classification accuracy obtained by using the FQ images alone can be explained as follows. It is possible that the MLC classification might not be the best method for classifying SAR images as compared to optical Landsat-5 TM images, since MLC assumes a normal distribution. The normal distribution fits the case of Landsat data while SAR data have a more complex distribution. As well, even though two dates were chosen, they were acquired under similar conditions; perhaps considering two FQ images acquired under contrasting conditions may have been more useful. With Radarsat-2 FQ SAR images, Shelat et al. (2012) showed that using contrasting FQ1 (18.52°-20.34°) and FQ20 (39.30°-40.74°) images and classified with MLC gave the highest overall accuracy for land cover classes in a tundra environment.

With Random Forests, when all fourteen FQ images with all four polarizations (HH, HV, VH and VV) were classified, the overall cross-validation result was 98.3%, which was not very different than when the Landsat-5 TM image was combined with the best FQ image pair (98.6%). Both of these cases gave better accuracies than using only the three polarizations of the FQ22/27 image pair (86.7%). This may indicate that while the use of Landsat does add to the accuracy, a similar accuracy may be achieved by using only FQ images acquired in variable incidence angle, leaf and moisture conditions. Being able to use solely SAR images rather than needing to use Landsat-5 TM images is of great interest. Indeed, for the study area, there was only one completely cloud-free and snow-free Landsat-5 TM image available from the vegetation season in 2011. In the case of the FQ/Landsat combination classification, the most important variables were Landsat TM4 (near infrared) and TM3 (red) bands, followed by the HH polarization, and the HV polarization of the FQ27 (dry, leaf-off) image. The least important variables were the two short-wave infrared Landsat bands (TM5 and TM7). Landsat TM4, TM3 and C-HH and HV images are all sensitive to the presence of vegetation in the imaged area. Indeed, TM4 and TM3 bands are sensitive to the chlorophyll activity of the vegetation. C-HV polarized images detect the significant depolarization and volume scattering occurring with vegetated areas (Evans et al., 1986, Greeley and Blumberg, 1995; Blumberg, 1998; del Valle et al., 2010).

Similar to the MLC classifier, adding the slope information in the classification had a lower effect on the classification accuracy of land cover types than did the addition of the Landsat opticaldata. When slope was combined with the FQ22/27 image pair, the overall cross-validation result increased from 86.7% to 90.8%. When the Landsat-5 TM image was added to the classification, the overall cross-validation result increased to 98.7%. Such results were already observed when classifying SAR images using Radarsat-1 C-HH SAR images (Grunsky et al., 2009), Radarsat-2 C-HH and C-HV images (LaRocque et al., 2012) and multi-polarized Radarsat-2 SAR images (Shelat et al., 2012).

5.4. Individual class accuracy

This section shall discuss the individual class accuracy for the Random Forests classifier only, as it is the one which gives the highest overall accuracy for any image combination (Table 15). Overall, for the non-water classes, the highest class accuracy was obtained for the *hardwood forest* class whatever the image combination, except for the one that combined the FQ image pair with the slope data, for which the highest class accuracy was obtained for the *softwood forest* class (Table 13).

It is the *open wetlands* class that had the lowest class accuracy for all classifications, except the one that combined the FQ image pair with the slope data, for which the lowest class accuracy was obtained for the *harvest area* class. The main confusion for open wetlands was with *low vegetation, bare soil*, and *softwood forests* classes. Under dry conditions, some of these open wetlands may have been dried out, thus explaining the backscattering similarities with the *low vegetation* class, both having short vegetation. The *closed wetland* class showed the most confusion with *softwood forests* and *open wetlands.*

The greatest class accuracy increase occurred for the *open wetlands* and *bare soil* classes when adding the Landsat data to the FQ image pair. However, the classified image obtained from the combination of an FQ image pair with the Landsat and slope data, showed that the *closed wetlands* have most likely been over-classified (Figure 7) as compared to the classified image produced from all fourteen FQ images (Figure 8). Indeed, confusion between *closed wetlands* and *hardwood forests* exists, mainly because closed wetlands are hardwood swamps, covered with maples (Figure 3), which may cause them to have similar reflectance. Such over-classification appears not to happen when using only the FQ images. The reason for this may be that these images better discriminate the presence of water below the canopy. It should be mentioned that for both wetland types, the study area comprises a limited number and size of wetlands. By having larger wetland areas, the training polygons would less likely be influenced by mixed pixels around the edges of the training areas. Further work is needed to test these algorithms in areas having large wetland areas.

5.5 Polarimetric variables and decompositions

Classification with the polarimetric variables had the lowest overall cross-validation results. However, the most important polarimetric variables were identified by referring to Random Forests variable importance. From the leaf-off dry FQ22 and FQ27 images, the six variables that appeared in the top ten most important are presented in Table 15.

Table 16. Most important polarimetric parameters from the Random Forests classification of the FQ 22 and FQ 27 polarimetric SAR images acquired under dry and leaf-off conditions

Type	Variable
Freeman-Durden decomposition	Power contribution due to volume scattering
Cloude-Pottier decomposition	Beta Angle
	Anisotropy
Touzi	Tau Angle
	Alpha_S Parameter
Polarimetric variable	Orientation angle for maximum of the completely polarized component

Table 16 shows that the incoherent target decompositions are the most important polarimetric variable in classification, as the only other variable that appears as important from both classifications is the orientation angle for the maximum of the completely polarized component. It would be interesting in the future to run a classification using Radarsat-2 HH, HV, VH and VV data, and Freeman-Durden (Freeman & Durden, 1998), Cloude-Pottier (Cloude & Pottier, 1997), and Touzi (Touzi, 2007; Touzi et al., 2007) decompositions.

6. Conclusions

This study examines the potential for using multi-beam Radarsat-2 C-Band polarimetric SAR, Landsat-5 TM, and DEM data for classifying wetland and non-wetland classes in a forested watershed in Ontario, Canada. It investigates the influence of incidence angle, leaf presence and moisture conditions in the classification of SAR images. The images were classified using two classification methods: the Maximum Likelihood Classifier (MLC) and Random Forests classifier. Lastly, SAR polarimetric variables and decompositions were investigated for their usefulness in classification.

The study showed that combining multi-beam Radarsat-2 C-band SAR data, Landsat-5 TM data, and slope from a DEM produced higher classification accuracy when mapping wetland areas over a forested watershed than Radar alone. It also highlighted the benefit of using multi-polarized (HH, HV, VV) over single polarization (HH) SAR imagery.

One of the most significant variables in the classification is the presence/absence of leaves during the time of image acquisition. For all SAR images, the leaf-off images produced higher cross-validation accuracies than leaf-on images, regardless of incidence angle or moisture conditions. Another factor that was investigated was the incidence angle. There was indication that steeper incidence angle was better in leaf-off conditions, however for leaf-on conditions, a conclusion could not be drawn. Lastly, dry conditions seem to be better than wet conditions. However, optimal conditions appear to be leaf-off, with a mix of incidence angle and moisture conditions for the Radarsat-2 C-band SAR images used in this study.

It was found that Random Forests produced higher classification accuracies than MLC for all image combinations. Random Forests also was beneficial in identifying which images are the most important in the classification of wetlands. When all fourteen multi-polarized SAR images were classified together, it showed that the leaf-off condition was the most important factor, and that a mix of incidence angles, moisture conditions, and polarizations (HH and VV) was important.

Polarimetric variables on their own did not provide good classification accuracies. However, with Random Forests, the most important polarimetric variables were identified, which were orientation angle for the maximum of the completely polarized component as well as others such as the Cloude–Pottier, Touzi, and Freeman-Durden decompositions. Combining these polarimetric variables with multi-polarized (HH, HV, VH, and VV) intensity images may be interesting in future studies.

Acknowledgments

Support for this research was provided by Kara Webster and Natural Resources Canada (Contract #3000445203), by a NSERC Discovery Grant awarded to Brigitte Leblon and by a TRANSFOR-M scholarship funded by Human Resources and Development Skills Canada. Contributions and guidance from Brigitte Leblon, Kara Webster and Heather Reese, as supervisors has been greatly appreciated. Thanks also go to Armand LaRocque, and Alessandro Montaghi, for data processing advice and assistance. Lastly, I would like to thank Tom Beckley, Håkan Olsson, and Johan Fransson for their support.

References

Augusteijn, M. and Warrender, C., 1998. Wetland classification using optical and radar data and neural network classification. International Journal of Remote Sensing, 19: 1545–1560.

Baghdadi, N., Bernier, M., Gauthier, R., and Neeson, I., 2001. Evaluation of C-band SAR Data for wetlands mapping. International Journal of Remote Sensing, 22(1): 71-88.

Blumberg, D.G. 1998. Remote sensing of desert dune forms by polarimetric synthetic aperture radar (SAR), Remote Sensing of Environment, 65: 204-216.

Bourgeau-Chavez, L., Kasischke, E., Brunzell, S., Mudd, J., Smith, K. and Frick, A., 2001, Analysis of space-borne SAR data for wetland mapping in Virginia riparian ecosystems. International Journal of Remote Sensing, 22: 3665–3687.

Castañeda, C. and Ducrot, D. 2009. Land cover mapping of wetland areas in an agricultural landscape using SAR and Landsat imagery, Journal of Environmental Management 90: 2270-2277.

Canadian Centre for Remote Sensing (CCRS). 2008, Radar Polarimetry, Natural Resources Canada, Accessed May 2012: http://www.nrcan.gc.ca/earth-sciences/geography-boundary/remote-sensing/fundamentals/1025.

Canadian Centre for Remote Sensing (CCRS). N.d, Radar Polarimetry, Advanced Radar Polarimetry Tutorial, Accessed May 2012: http://www.nrcan.gc.ca/earth-sciences/geography-boundary/remote-sensing/radar/1893.

Canadian Space Agency (CSA). 2007. RADARSAT-2. Accessed May 2012: http://www.asc-csa.gc.ca/eng/satellites/radarsat2/.

Cloude S.R., Pottier E. 1997. An entropy based classification scheme for land applications of polarimetric SAR. IEEE Transactions on Geoscience and Remote Sensing, 35(1):68-78.

Congalton, R. 1991. A review of assessing the accuracy of classifications of remotely sensed data. Remote Sensing of Environment, Vol. 37, pp. 35–46.

Cox, K.W. 1993. Wetlands A celebration of life. Sustaining Wetlands, Issues Paper, No 1993-1 Cat . No. CW6Cr125/1993E.

Crevier, Y., Pultz, T.J., 1996. Analysis of C-band SIR-C/X Sar Radar Backscatter Over a Flooded Environment, Red River, Manitoba, Proc. 3rd International Symposium on Applications of Remote Sensing in Hydrology; p. 47-60.

del Valle, H.F., Blanco, P.D., Metternicht, G.I., and Zinck, J.A. 2010. Radar remote sensing of wind-driven land degradation processes in northeastern Patagonia. Journal of Environmental Quality, Vol. 39, pp. 62-75.

Evans, D.L., T.G. Farr, J.P. Ford, T.W. Thompson, C.L. Werner. 1986. Multipolarization radar images for geologic mapping and vegetation discrimination, IEEE Transactions on Geoscience and Remote Sensing, 24(2): 246-257.

Freeman A., and Durden S.L. 1998. A three-component scattering model for polarimetric SAR data. IEEE Transactions on Geoscience and Remote Sensing, 36(3): 963- 973.

Gislason, P., Benediktsson, J., and Sveinsson, J. 2006. Random Forests for land cover classification. Pattern Recognition Letters 27: 294-300.

Goodman J.W. 1976. Some fundamental properties of speckles. Journal of Optical Society of America, Vol. 66, No. 11, pp. 1145-1150.

Greeley, R., and Blumberg D.G. 1995. Preliminary analysis of Shuttle Radar Laboratory (SRL-1) data to study aeolian features and processes. IEEE Transactions on Geoscience and Remote Sensing, Vol. 33, No.4, pp. 927-933.

Grings, F.M., Ferrazzoli, P., Jacobo-Berlles, J.C., Karszenbaum, H., Tiffenberg, J., Pratolongo, P. and Kandus, P., 2006, Monitoring flood conditions in marshes using EM models and Envisat ASAR observations. IEEE Transactions on Geoscience and Remote Sensing, 44: 936–942.

Grunsky, E.C., Harris, J.R., and McMartin, I. 2009. Predictive mapping of surficial materials, Schultz Lake area (NTS 66 A), Nunavut, Canada. Reviews in Economic Geology, Vol. 16, pp. 177-198.

Henderson, F., and Lewis, A. 2008. Radar detection of wetland ecosystems: a review. International Journal of Remote Sensing, Vol. 29, No. 20, 5809-5835.

Henry, J., Chastanet, P., Fellah, K. and Desnos, Y., 2006, Envisat multi-polarized ASAR data for flood mapping. International Journal of Remote Sensing, 27: 1921– 1929.

Hess, L., Melack, J. and Simonett, D., 1990. Radar detection of flooding beneath the forest canopy: a review. International Journal of Remote Sensing 11:1313–1325.

Kandus, P., Karszenbaum, H., Pultz, T., Parmuchi, G., and Bava, J., 2001, Influence of flood conditions and vegetation status on the radar backscatter of wetland ecosystems. Canadian Journal of Remote Sensing, 27, p 651-662.

Kasischke, E. and Bourgeau-Chavez, L., 1997. Monitoring south Florida wetlands using ERS-1 SAR imagery. Photogrammetric Engineering and Remote Sensing 63: 281–291.

LaRocque, A., Leblon, B., Harris, J., Jefferson, C., Tschirhart, V., Shelat, Y. 2012. Surficial materials mapping in Nunavut, Canada with multibeam RADARSAT-2 dual-polarization C-HH and C-HV, LANDSAT-7 ETM+, and DEM data. Canadian Journal of Remote Sensing, 38(3):281-305.

Leblon, B., 1999 Mapping forest clearcuts using radar digital imagery: A review of the Canadian experience. The Forestry Chronicle, Vol 75, No. 4, 675-684.

Leconte, R., and Pultz, T., 1991, Evaluation of the potential of RADARSAT for flood mapping using simulated satellite SAR imagery. Canadian Journal of Remote Sensing, 17:241-249.

Lee J.S., Grunes, M.R., Kwok R. 1994. Classification of multi-look polarimetric SAR imagery based on the complex Wishart distribution. International Journal of Remote Sensing, 15(11):2299-2311.

Lee J.S., Grunes M.R., de Grandi, G. 1999. Polarimetric SAR speckle filtering and its implication for classification, IEEE Transaction on Geoscience and Remote Sensing, 37(5): 2363-2373.

Li, J., and Chen, W., 2005. A rule-based method for mapping Canada's wetlands using optical, radar and DEM data, International Journal of Remote Sensing. Vol. 26, No.22, 5051-5069 DOI:10.1080/01431160500166516

Lillesand, T., Kiefer, R., and Chipman, J. 2008. Remote Sensing and Image Interpretation 6th Edition, John Wiley & Sons, Inc.

Michelson, D., Liljeberg, B., Pilesjö, P. 2000. Comparison of Algorithms for Classifying Swedish Landcover Using Landsat TM and ERS-1 SAR Data, Remote Sensing of Environment. 71:1-15.

National Wetlands Working Group. 1988. *Wetlands of Canada*. Ecological Land Classification Series, No. 24. Environment Canada and Polyscience Publications Inc. Ottawa, Ontario. 452 p.

National Wetlands Working Group. 1997. The Canadian Wetland Classification System, 2nd Edition, Wetlands Research Centre, University of Waterloo, Waterloo, Ontario.

Ozesmi, S. L., and Bauer, M. E., 2002. Satellite remote sensing of wetlands, Wetland Ecology and Management 10: 381- 402.

Pedroni, l., 2003. Improved classification of Landsat Thematic Mapper data using modified prior probabilities in large and complex landscapes, International Journal of Remote Sensing, Vol 24, No 1, pp 91 – 113.

Pope, K., Rejmankova, E., Paris, J. and Woodruff, R., 1997. Detecting seasonal flooding cycles in marshes of the Yucatan peninsula with SIR-C polarimetric radar imagery. Remote Sensing of Environment 59:157–166.

R Development Core Team, 2012. R: A language and environment for statistical computing. R Foundation for Statistical Computing, Vienna, Austria. ISBN 3-900051-07-0, URL http://www.R-project.org/.

Ramsey, E. W. 1998. Radar remote sensing of wetlands *IN* Remote Sensing Change Detection: Environmental Monitoring Methods and Applications. Eds. R.S. Lunetta and C.D Elvidge. Chelsea: Sleeping Bear Press, Inc. 318p.

Ramsey, E., III, Nelson, G., Sapkota, S., Laine, S., Verdi J. and Krasznay, S., 1999, Using multiple-polarization L-band radar to monitor marsh burn recovery. IEEE Transactions on Geoscience and Remote Sensing 37:635–639.

Ramsey, E., Rangoonwala, A., Middleton, B., Lu, Z. 2009. Satellite optical and radar data used to track wetland forest impact and short-term recovery from Hurricane Katrina, WETLANDS, Vol. 29, No. 1, pp. 66-79.

Reese, H. 2011. Classification of Sweden's Forest and Alpine Vegetation Using Optical Satellite and Inventory Data, Doctoral Thesis No. 2011:86, Faculty of Forest Science, Swedish University of Agriculture Science, Umeå.

Shelat, Y., Leblon, B., LaRocque, A., Harris, J., Jefferson, C., Lentz, D., and Tschirhart, V., 2012. Effects of incidence angles and image combinations on mapping accuracy of surficial materials in the Umiujalik Lake area, Nunavut, using RADARSAT-2 polarimetric and LANDSAT-7 images, and DEM data. Part 1. Nonpolarimetric analysis. Canadian Journal of Remote Sensing, 38(3):383-403.

Sokol J., NcNairn H., and Pultz T.J. 2004. Case studies demonstrating hydrological applications of C-band multi-polarized and polarimetric SAR, Canadian Journal of Remote Sensing, 30(3): 470-483.

Townsend, P.A. 2002. Relationships between forest structure and the detection of flood inundation in forested wetlands using C-Band SAR, International Journal of Remote Sensing, 23(3), pp. 443-460.

Touzi, R., 2007. Target Scattering Decomposition in Terms of Roll-Invariant Target Parameters. IEEE Transaction on Geoscience and Remote Sensing, Vol. 45 no 1.

Touzi, R., Deschamps, A. Rother, G. 2007. Wetland characterization using polarimetric RADARSAT-2 capability, Canadian Journal of Remote Sensing, 33(1): S56-S67.

Wang, Y., Hess, L., Filsos, S. and Melack, J., 1995, Understanding the radar backscattering from flooded and nonflooded Amazonian forests: results from canopy backscatter modeling. Remote Sensing of Environment, 54:324–332.

Wang, J., Shang, J., Brisco, B., and Brown, R., 1998, Evaluation of multidate ERS-1 and multispectral Landsat imagery for wetland detection in Southern Ontario. Canadian Journal of Remote Sensing, 31, pp.214-224.

Waske, B., Braun, M. 2009. Classifier ensembles for land cover mapping using multitemporal SAR imagery, ISPRS Journal of Photogrammetry and Remote Sensing, 64 pp. 450-457.

Yamagata, Y. and Yasuoka, Y. 1993. Classification of wetland vegetation by texture analysis methods using ERS-1 and JERS-1 images, Proc. IGARSS'93, 4: 1614-1616.